Faculty Scholarship

1-2021

Non-Invasive Measure of Stenosis Severity Through Spectral Analysis [post-print]

Clayton P. Byers
Trinity College Hartford, clayton.byers@trincoll.edu

Alexandra Sinson
Trinity College, Hartford Connecticut, alexandra.sinson@trincoll.edu

Colette Scheffers
Trinity College, Hartford Connecticut, colette.scheffers@trincoll.edu

Taikang Ning
Trinity College, Hartford Connecticut, taikang.ning@trincoll.edu

Trinity College
HARTFORD CONNECTICUT

Non-Invasive Measure of Stenosis Severity Through Spectral Analysis

Clayton P. Byers
Department of Engineering
Trinity College
Hartford, USA
clayton.byers@trincoll.edu

Alexandra M. Sinson
Department of Engineering
Trinity College
Hartford, USA
alexandra.sinson@trincoll.edu

Colette M. Scheffers
Department of Engineering
Trinity College
Hartford, USA
colette.scheffers@trincoll.edu

Taikang Ning
Department of Engineering
Trinity College
Hartford, USA
taikang.ning@trincoll.edu

Abstract—A preliminary study on the effect of stenosis severity in a restricted flow is performed through the spectral analysis of sound signals. A model pulsatile flow that uses differing area reductions through an opening was employed, where contact microphones secured outside of the reduction measured the sound intensity in the flow. A spectral analysis shows the narrowing results in increased magnitude of frequencies in the range of 15 to $170 Hz$, with different narrowing cases resulting in different peak frequencies. Low frequency content up to $10\,Hz$ remains approximately unchanged. This simplistic approach of signal processing forms a basis for enhanced understanding and diagnosis of the severity of narrowing in an internal flow, and encourages future research into more complicated bispectral methods of analysis. The results show a clear difference between "regular" turbulence present in an internal flow and "enhanced" turbulence due to a stenosis or similar restriction in the flow.

Index Terms—stenosis, spectrum, internal flow

I. INTRODUCTION

A. Characterization of Stenosis

Aortic valve stenosis occurs when the heart's aortic valve narrows. This narrowing prevents the valve from opening fully. It is caused by calcification of the aortic valve leaflets. As such, it reduces or blocks blood flow from the left ventricle heart into the main artery (aorta) and the rest of the body. When the blood flow through the aortic valve is reduced or blocked, the heart needs to work harder to pump blood to the body. It is a common heart disease and its complication is potentially the most life-threatening [1]. During stenosis auscultation a murmur having a diamond shaped can be seen on the phonocardiograph. The murmur is caused by turbulent blood flow into the aorta with regular vibrations. In severe aortic stenosis there is a mid-systolic diamond shaped murmur that is loud and higher pitch than the murmur of mild aortic stenosis. Examples of mild and severe mid-systolic murmurs caused by aortic valve stenosis are shown in Fig. 1.

It is known that murmurs produced by severe aortic stenosis are louder with a higher pitch than the murmur of mild aortic stenosis. The systolic murmur intensity can be categorized by the Levine scale [2] from 1 to 6 to indicate its clinical significance. The murmur frequency is linked to turbulent blood flow, but the connection between the turbulence and the severity of
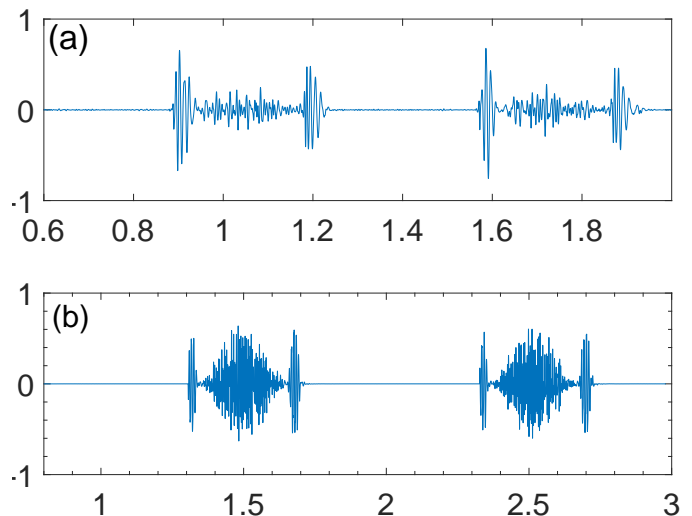
Fig. 1: Mid-systolic murmurs caused by aortic valve stenosis. Time in seconds is shown on the abscissa, while the ordinate is the magnitude of the sound signal. Mild severity shown in (a), severe shown in (b).

aortic value stenosis is often overlooked. This underlying study will use the power spectral analysis to characterize the murmur frequency that carries equally important clinical information for heart disease diagnosis.

B. Turbulence and Stenosis

Turbulence is characterized by chaotic fluctuations in the velocity field of a fluid flow, resulting in a distribution of kinetic energy that ranges throughout all scales, otherwise known as eddies, in the flow [3]. The intensity of the energy across these scales is often characterized through a spectral analysis. The power spectrum of a velocity signal would give an indication of the energy contained at the different scales, characterized by either wavenumber or frequency, in the flow at the location of this velocity signal. Increasing wavenumber or frequency corresponds to a decrease in eddy size, and there tends to be a corresponding decrease in overall energy contained in these smaller eddies.

Popular measurement techniques of turbulent flows often seed the flow with a passive scalar, which is tracked [4]. The motion of these seeding particles are assumed to follow that of the fluid particles, and therefore allow the researcher to directly measure the fluid motion. Non-invasive techniques must be employed to measure the instantaneous flow of blood in humans, restricting the methodology and preventing a direct observation of the flow velocity. One way this could be accomplished is through the use of pressure or vibration measurements. Obtaining a direct measure of the fluctuating pressure in a flow is a difficult prospect, but surface measurements of pressure are correlated with turbulence intensity [5]. This is easily shown through the Poisson equation of fluctuating pressure in an incompressible Newtonian fluid with constant density and viscosity as

$$\nabla^2 p = -\rho \left[2 \frac{\partial \overline{U}_i}{\partial x_j} \frac{\partial u_j}{\partial x_i} + \frac{\partial^2}{\partial x_i \partial x_j} \left(u_i u_j - \overline{u_i u_j} \right) \right], \quad (1)$$

where p is the fluctuating pressure, ρ is the fluid density, $\overline{U}_i$ is the mean velocity in the i direction, u_j is the instantaneous fluctuating velocity in the j direction, the Cartesian coordinate directions are denoted with x_i, an over-bar indicates an ensemble average, and the repeated indices indicate summation over the range of $i, j = 1, 2, 3$. The last term on the right hand side of (1) is known as the Reynolds stress, and is a measure of the correlation of velocity fluctuations within a flow. Higher values of $\overline{u_i u_j}$ are indicative of a more energetic turbulence in the flow, and the trace of the Reynolds stress is known as the turbulence kinetic energy, again a measure of the intensity of turbulence. Note that the pressure at a location on the wall is the result of an integral over space of (1), resulting in an intimate coupling of turbulence intensity and fluctuating pressure.

The nature of (1) results in the core region of a turbulent flow exerting significant influence over the wall pressure fluctuations [6], and recent studies have shown that coherent structures in wall-bounded flows are intimately tied to the wall pressure fluctuations, where differing filtering methodologies of the wall pressure can be used to identify wall-normal turbulent eddies of different size [7]. This indicates that measurements of the pressure (or analogous measurement) at the wall of an artery would allow an indication of the level and intensity of turbulence within the artery.

A recent study found that electronic stethoscopes are capable of detecting major coronary artery stenoses [8]. The introduction of turbulent eddies in the flow causes fluctuating stresses on the arterial wall, manifesting as pressure waves and acoustic vibrations [8]. Therefore, the measurement of these acoustic vibrations and a subsequent spectral analysis can provide an indication to the severity of turbulence within the flow. While it is commonly accepted that normal arterial blood flow is laminar [8], studies have shown that turbulence is more prevalent in blood flows than previously thought [9], [10]. This study will undertake an effort to differentiate between "regular" turbulence present in an internal flow and
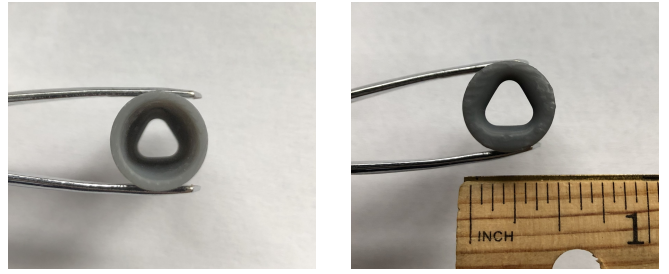

Fig. 2: Example of flow constricting geometry. Left picture shows the wider inlet, which tapers to a 20% area opening, seen on the left. Exit geometry was picked to roughly mimic an arterial valve.

"enhanced" turbulence due to a stenosis or similar restriction in the flow.

II. Experimental Setup

Human bodies have layers of skin, fat, and tissue, in addition to other organs that will influence and attenuate a vibration signal caused by turbulence in the arteries [11]. The experimental setup will reflect these limitations, where the measurements taken in this study are not a direct measurement of turbulence, but instead an indirect analog of the intensity of turbulence, where distinguishing characteristics of a sound signal are sought out to indicate the severity of the narrowing in the flow. A simple open-loop pulsatile flow device was created with the ability to swap out a different narrowing sections, as seen in Fig. 2. Sound pressure levels were measured using a contact microphone fixed to the surface of the tubing before and after the narrowing.

Arterial flow is pulsatile and therefore the characteristics of the flow will be periodic. The Reynolds number is used to characterize the dynamic parameters of a fluid flow, and is defined as:

$$Re = \frac{\rho U D}{\mu} \quad (2)$$

where D is a characteristic length scale (in this case the tube diameter) and μ is the viscosity of the fluid. Studies have found arterial blood flow has a Reynolds number that can average around $Re = 4000$ [12] and peak up to $Re = 10000$ [9]. The average Reynolds number in this experimental setup was measured to be $Re = 6400$.

A one-way hand pump was used to pulse the flow, which drew water from a reservoir and sent it through the opening, returning to the reservoir. The pump was held in a device to set the maximum compression, and thus flow rate, and the rate of pumping was held at $1\,Hz$. The narrowing section and contact microphones were physically isolated from the pumping mechanism to minimize additional vibration from the setup.

Three test cases were performed: a baseline test of zero reduction in area, a narrowing with 30% baseline area, and a severe narrowing of 20% baseline area. These signals were
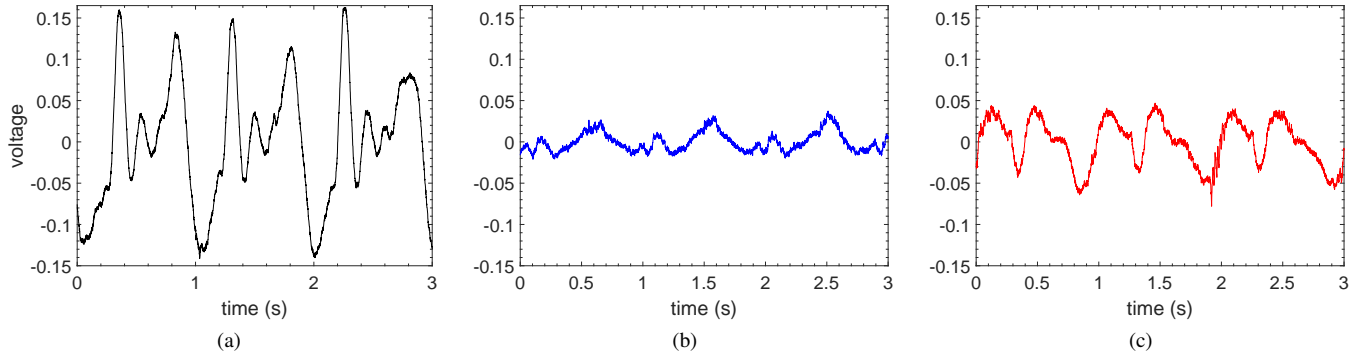
Fig. 3: Raw signal for each of the three cases. Baseline test with no restriction is shown in (a), 30% opening in shown in (b), and 20% opening is shown in (c).

recorded for 30 second intervals with four independent tests occurring for each case.

There are many proven power spectral estimation algorithms capable of displaying the energy distribution of a target signal in the frequency domain [13]. The power spectra of the collected data was computed using the fast Fourier transform (FFT) based periodogram. In particular, an overlapped segment averaging periodogram algorithm was used in this study to provide good statistical confidence. Experimental data were divided into shorter segments of 2.5-second duration where adjacent segments were overlapped by 50%. Each data segment was multiplied by a Hanning tapering function to provide smooth transition near segment edges.

III. RESULTS

An excerpt of the raw signal for each of the three cases is shown in Fig. 3. Each signal has been centered on zero to show the time-dependent variation, and noise reduction has been utilized to remove an unwanted $60\,Hz$ interference. The periodicity of each signal is apparent, with the pumping action seen to occur approximately three times in the three second period, corresponding to the $1\,Hz$ pumping frequency.

It is apparent that each signal has a different amplitude, preventing a one-to-one comparison of the raw signals. One reason for this difference is due to the restrictions changing the volume flow within the tubing, thus altering the overall turbulence intensity (which is related to the Reynolds stress) and therefore sound amplitude. When performing the spectral analysis, the power spectrum of each signal will be normalized by the signal variance:

$$\phi_n(f) = \frac{P_n(f)}{\sigma_n^2}$$

where ϕ_n is the normalized spectrum of the nth case, $P_n(f)$ is the power spectrum of the voltage for case n, f is the frequency in Hz, and σ_n^2 is the variance of the nth signal. This normalization will allow interpretation of the results relative to one another, regardless of the amplitude of each signal.

The normalized spectrum for each signal is shown in Fig. 4. The $60\,Hz$ noise reduction for the signals does not completely

remove all influence from the original noise, as can be seen in each of the three cases. The baseline case, shown in Fig. 4a, has a small added energy at $60\,Hz$ but has otherwise shown complete removal of the remaining influence of the external electrical noise. The two narrowed cases both show a little more influence from the $60\,Hz$ electrical noise, in addition to some harmonics at 120 and $180\,Hz$. For all three cases, the immediate regions around these three frequencies will be ignored due to the inability to distinguish between enhanced turbulence from the stenosis and the electrical noise. Additionally, all three cases had no significant change in the spectrum present above $200\,Hz$. Therefore, all data will be truncated at this value.

Inset in Fig. 4a are all three signals at the low frequency limit. It is apparent that each case has the same fundamental $1\,Hz$ pumping frequency and harmonics of it, and each case follows nearly the same trend up to approximately $8\,Hz$. This indicates that for the same fundamental pumping rate, different restrictions to the flow do not induce any significant change to the low frequency energy distribution in the flow.

The baseline case shows a consistent decrease in energy as the frequency increases. The existence of this energy spectrum is indicative of turbulence in the baseline case, which should be expected for the given Reynolds number of $Re = 6400$, which is above the fully turbulent $Re = 4000$ for pipe flow. At higher Reynolds numbers, the relative amount of energy at each frequency would be expected to increase, and the range of frequencies containing significant amounts of energy would likewise be expected to increase. Both restricted cases in Fig 4b and Fig. 4c show the normalized spectrum contains a greater amount of energy at all frequencies compared to the baseline. This is indicative of enhanced turbulence in the flow, as the increase in sound pressure level is tied to turbulence intensity.

Regarding the influence of stenosis severity on the frequencies present, Fig. 4b shows a vibration caused by turbulence appearing near $30\,Hz$ in the 30% opening. As the restriction becomes more narrow (the 20% case in Fig. 4c), the turbulent vibration energy shifts towards $50\,Hz$. Other prominent peaks
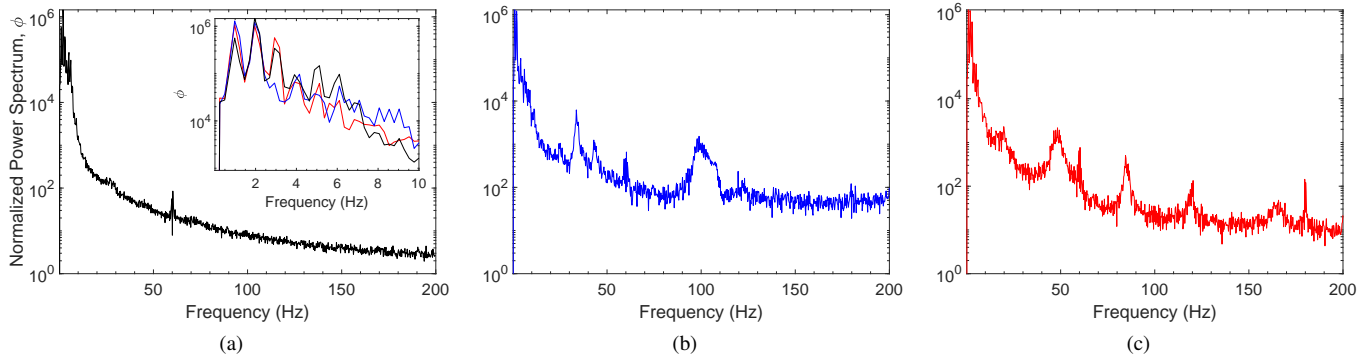
Fig. 4: Normalized Spectrum ϕ for each of the three cases. Baseline test with no restriction shown in (a), 30% opening shown in (b), and 20% opening shown in (c). Inset in (a) shows the three cases at the low frequency limit.

in energy are summarized below.

The 30% area case, shown in Fig. 4b, has three prominent peaks: one at $33\,Hz$, a smaller one at $43\,Hz$, and a broader region centered on $100\,Hz$. Also of note is the higher frequency region ($f > 100\,Hz$) has a larger overall energy than either the baseline or the 20% area case. This is likely due to an overall increase in turbulence associated with higher Reynolds numbers, but further study is needed for definitive conclusions.

The 20% area case, shown in Fig. 4c, has four prominent regions of increased energy: a slight bump at $20\,Hz$, two wider regions centered around 48 and $84\,Hz$, and one slight increase centered on $165\,Hz$. Again, the peaks at 60, 120, and $180\,Hz$ are likely due to the electrical noise, even after noise reduction measures were taken.

Another method to visualize the frequencies of influence in which energy has been enhanced is to add the energy content over a range of frequencies and compare these bins of data for each case. Enhanced energy content will show as a larger magnitude for a given bin, indicating some mechanism is generating energy in those range of frequencies. Table I shows the change in normalized energy content, relative to the baseline case, in given frequency bands. The selected bands showed a significant change in energy content relative to both the baseline case and surrounding frequency bands, and therefore serve as a predictive frequency range indicative of a narrowing or stenosis in the flow. Note the low frequencies of

TABLE I: Relative change in energy compared to the unrestricted baseline case for given frequency bands.

Frequency	Relative Energy Change	
Band (Hz)	30% *opening*	20% *opening*
$0 - 10$	1.02	0.99
$15 - 25$	3.57	**5.58**
$30 - 40$	**19.1**	3.19
$40 - 60$	9.00	**16.8**
$80 - 90$	6.71	**11.9**
$90 - 110$	**58.5**	2.94
$160 - 170$	13.0[a]	**8.19**

[a]Not significantly different from surrounding values

$0 - 10\,Hz$ show nearly identical normalized energy content in each case, as evidenced in the inset of Fig. 4a.

As previously discussed, the introduction of the narrowing in the flow enhances turbulence, resulting in greater overall energy at all frequencies in the flow. This is evident from Fig. 4 for both cases relative to the baseline. The 30% opening can be characterized by the frequency band around 30 to $40\,Hz$, whose magnitude is 19.1 times greater than the baseline case, and at 90 to $110\,Hz$, with a $58.5-$fold increase in magnitude. Both of these frequency bands also have a significantly higher energy compared to the 20% case. Note that the $160 - 170\,Hz$ band has a similar relative magnitude to the surrounding bands, and therefore is not a significant indicator. For the 20% opening, the $15 - 25$, $40 - 60$, and $80 - 90\,Hz$ bands all demonstrate a higher energy content relative to the baseline, the surrounding frequencies, and the 30% opening. Note that $160 - 170\,Hz$ band has a significant increase in energy relative to the baseline and surrounding frequencies, but has a smaller magnitude of increase compared to the 30% case.

IV. CONCLUSIONS AND FUTURE WORK

The two cases with a reduction of area demonstrated significant increases in relative energy at given frequency bands compared to the baseline case, indicating audible frequencies that differentiate the behavior between the severity of stenosis. Both restrictions enhanced the overall turbulence in the flow, resulting in an increase in energy across the spectrum relative to the baseline. The first prominent frequency shifts to higher values as the severity of the narrowing increases.

It has previously been shown that acoustic signals would be present in stenosis cases of at least 50% area reduction [8], which is consistent with our limited cases. However, research has shown that patients with stenosis show significant energy contained at higher frequencies than found in this study [8]. The simplified geometry, rigid material properties of the narrowing, and constant viscosity of this model setup will all contribute to the limitation of frequencies observed. Nonetheless, the range of predictive frequencies of arterial stenosis [9] encompass the frequencies found to be most excited in the two restricted cases.

Future modifications and testing will account and control the variation in flow rates and overall sound amplitude with more accurate real-time measurements of the flow rate. While normalization of the spectrum allowed a comparison of the dominant frequencies present, a better attempt at matching the overall dynamic parameters of the flow, such as bulk Reynolds number, will further emphasize the similarities and differences in the vibrations within the flow.

Advanced signal processing techniques will be utilized in future studies, such as a cross-spectrum analysis [14] or bispectral analysis [15]. These techniques would allow further insight into the relationship between dominant frequencies present in restricted cases, enhancing the capability of stenosis severity detection through acoustic measurements.

Another open area of investigation lies in the coupling of turbulent flow and buffeting or flutter of the arterial valve leading to enhanced vibrational energy. This preliminary study does not differentiate between their effects, but future work could include narrowing devices made of flexible materials to study their effects.

REFERENCES

[1] B. A.Carabello, W. J. Paulus "Aortic stenosis," *The Lancet*, vol. 373 no 9667, pp. 956-966. Mar 2009

[2] M.E. Silverman, C. F. Wooley, "Samuel A. Levine and the history of grading systolic murmurs," *Am. J Cardiol.*, vol. 102, no. 8, pp. 1107-1110. Oct 2008.

[3] H. Tennekes, and J.L. Lumley, *A First Course in Turbulence*. Cambridge, MA, USA: MIT press, 1972.

[4] R.J. Adrian, "Twenty years of particle image velocimetry," *Exp. Fluids* vol. 39, pp. 159–169, Jul. 2005.

[5] W.W. Willmarth, "Pressure fluctuations beneath turbulent boundary layers," *Ann. Rev. Fluid Mech.*, vol. 7, no. 1, pp. 13-36, Jan. 1975.

[6] T.M. Farabee, and M.J. Casarella, "Spectral features of wall pressure fluctuations beneath turbulent boundary layers," *Phys. Fluids A: Fluid Dyn.* vol. 3, no. 10, pp. 2410-2420, Oct. 1991.

[7] C.S. Vila, and O. Flores, "Wall-based identification of coherent structures in wall-bounded turbulence," *J. Phys.: Conf. Series*, vol. 1001, No. 1, 2018.

[8] F. Azimpour, E. Caldwell, P. Tawfik, S. Duval, and R.F. Wilson, "Audible coronary artery stenosis," *Amer. J. Medicine* vol. 129, no. 5, pp. 515-521, May 2016.

[9] P.D. Stein, and H.N. Sabbah, "Turbulent blood flow in the ascending aorta of humans with normal and diseased aortic valves," *Circulation Res.*, vol. 39, no. 1, pp. 58-65, Feb. 1976.

[10] Duo Xu el al., "Nonlinear hydrodynamic instability and turbulence in pulsatile flow," *Proc. Nat. Academy Sciences*, vol. 117, no 21, pp. 11233-11239, May 2020.

[11] J.F. Sangster, and C.M. Oakley, "Diastolic murmur of coronary artery stenosis," *Brit. Heart J.*, vol 35, pp. 840-844, 1973.

[12] A. Mahalingam, et al., "Numerical analysis of the effect of turbulence transition on the hemodynamic parameters in human coronary arteries," *Cardiovascular diagnosis and therapy*, vol. 6, no. 3, pp. 208-220, Jun. 2016.

[13] S. M. Kay, and S. L. Maple, Jr., "Spectrum analysis-a modern perspective," *Proc. IEEE*, Vol. 69, No. 11, pp. 1380-1419, Nov 1981.

[14] G. C. Carter, C. Knapp, A. Nuttall, "Estimation of the magnitude-squared coherence function via overlapped fast Fourier transform processing," *IEEE Trans. Audio Electroacoust.*, vol. 21, no. 4 pp. 337-344, Aug. 1973.

[15] T. Ning and J. D. Bronzino, "Bispectral analysis of the rat EEG during various vigilance states," *IEEE Trans. Biomed. Eng.*, vol. 36, no. 4, pp. 497-499, April 1989.